NANO LETTERS

2007
Vol. 7, No. 9
2865−2870

Biodistribution of Quantum Dot Nanoparticles in Perfused Skin: Evidence of Coating Dependency and Periodicity in Arterial Extraction

Hyun A. Lee,[†,‡] Mudassar Imran,[†,‡] Nancy A. Monteiro-Riviere,[‡] Vicki L. Colvin,[§] William W. Yu,[§] and Jim E. Riviere*[,†,‡]

Center for Chemical Toxicology Research and Pharmacokinetics, and Biomathematics Program, North Carolina State University, 4700 Hillsborough Street, Raleigh, North Carolina 27606, and Department of Chemistry, Center for Biological and Environmental Nanotechnology, Rice University, Houston, Texas

Received June 29, 2007; Revised Manuscript Received July 24, 2007

ABSTRACT

Arterial extraction of quantum dots (QD) assayed by fluorescence or inductively coupled plasma (ICP) emission spectrometry were studied after infusion into isolated perfused skin. Extraction was mathematically modeled using three linear differential equations. COOH-coated QD had greater tissue deposition, assessed both by model prediction and laser confocal scanning microscopy, than did QD-PEG. Both QD had a unique periodicity in arterial extraction never observed with drug infusions, suggesting a potentially important nanomaterial behavior that could affect systemic disposition.

There has been explosive growth in the study of nanomaterials for applications in fields ranging from biomedicine to microelectronics.[1,2] Knowledge of the disposition and pharmacokinetics of nanomaterials in tissues is important for both developing nanotechnology-based drug delivery systems as well as conducting realistic risk assessments.

There is minimal literature on the pharmacokinetics of nanomaterials, with that available being focused on therapeutic applications. A classic pharmacokinetic study was conducted in Sprague−Dawley rats using MSAD-C_{60}, a water-soluble C_{60} derivative with antiviral properties.[3] Distribution of ^{99m}Tc labeled $C_{60}(OH)_x$ in mice and rabbits after iv dosing occurred in the kidney, bone, spleen, and liver with slow elimination after 48 h, except for bone, which accumulated the label.[4] Rigorous, "classical" pharmacokinetic studies on other nanomaterials have not been conducted.[5] The few reported studies have employed indirect measures of concentration (IR,[6] PET[7]) or particles functionalized with specific tracers.[8] Literature exists on nanomaterial deposition after inhalational exposure, primarily on local deposition within the respiratory tract.[9,10] Knowledge of how absorbed particles distribute in other tissues is lacking.

QD are semiconductor nanocrystals whose properties make them good candidates for application ranging from diagnostic imaging to solar cells.[11,12] QD are heterogeneous nanoparticles that consist of a colloidal core surrounded by one or more surface coatings. The surface coating can prevent agglomeration, encapsulate toxic metals, affect absorption and transport, modulate immunological responses, modify or prevent toxicity, and assist in tissue elimination. Coatings are frequently applied to customize QD for specific applications.[13−16] QD are readily detected because of their intense and photostable fluorescence, making them a useful model for assessing nanomaterial interactions with biological systems. A pharmacokinetic study of intravenous QD 705 in mice demonstrated a relatively short plasma half-life of 18.5 h but persistent and even increasing tissue concentrations and tissue redistribution for up to 28 days.[17]

Water-soluble QD were synthesized as previously reported.[18,19] QD core/shell structures were synthesized based on the literature, but the CdS shell growth temperature was adjusted to 180 °C (CdSe as the core).[20] These QD were purified and stored in chloroform. QD concentrations were determined using the available extinction coefficients.[21] For amphiphilic polymers, we used poly(maleic anhydride-*alt*-1-octadecene) (PMAO, M_n = 30 000−50 000, Aldrich)

* Corresponding author. E-mail address: Jim_Riviere@ncsu.edu. Telephone: 919-513-6305. Fax: 919-513-6358.

[†] Center for Chemical Toxicology Research and Pharmacokinetics, North Carolina State University.

[‡] Biomathematics Program, North Carolina State University.

[§] Department of Chemistry, Center for Biological and Environmental Nanotechnology, Rice University.

10.1021/nl071563c CCC: $37.00
Published on Web 08/09/2007

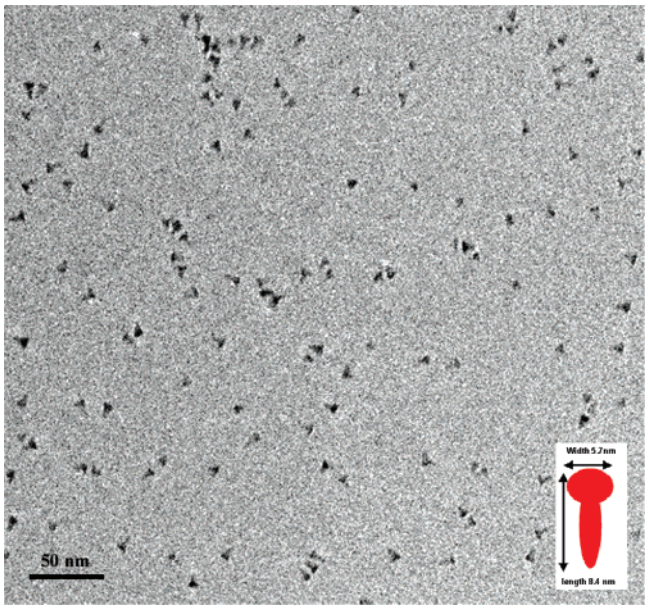

Figure 1. Dry TEM of a QD-PEG 621.

reacted with a amino poly(ethylene glycol) methyl ether (mPEG-NH_2, MW 6000; Nektar, CA) in chloroform overnight to form amphiphilic polymers (PMAO-PEG) (molar ratios of PMAO:PEG were 1:5 and 1:30, respectively, for negative and neutral water-soluble QD). These PMAO-PEG amphiphilic polymers were used to transfer the QD into aqueous phases. For water-soluble nanocrystals, the QD and PMAO-PEG were mixed in chloroform and stirred for 1 h (molar ratio of QD:PMAO-PEG was 1:10). Then the water was added in the same volume of the chloroform solution; chloroform was removed by rotary evaporation and resulted in a clear and colored solution of water-soluble QD. An ultracentrifuge (Beckman Coulter Optima L-80XP) was used to concentrate and purify (remove excess amphiphilic polymer) the materials (typically at 200 000−300 000 g for 1−2 h). Ultraviolet visible absorption spectra of QD were measured by a Varian Cary 5000 spectrophotometer, which showed the first excitonic absorption peak of 615 nm. Photoluminescence (PL) spectra of QD were recorded on a Jobin Yvon Spex Fluorolog 3 fluorescence spectrophotometer with a peak position of 621 nm. The quantum yield was then measured as 54% using R6G as the reference. Transmission electron microscopy (TEM) specimens were made by evaporating one drop of nanocrystal solution on a carbon-coated copper grid. The TEM micrographs were taken on a JEOL FasTEM 2010 microscope operating at 100 kV. The size and size distribution data were obtained by counting >1000 individual nanocrystalline particles using Image-Pro Plus 5.0 (Media Cybernetics Inc.).[22,23] The size for the inorganic CdSe/CdS was about 8.4 nm × 5.8 nm (Figure 1). The overall hydrodynamic size of both water-soluble QD was about 39−40 nm.[19] For the neutral QD, PEG molecules completely covered the structure, whereas the negatively charged QD had less PEG molecules, so the free COOH groups (generated when reacted with amino groups in PEGs and with water) had greater access.

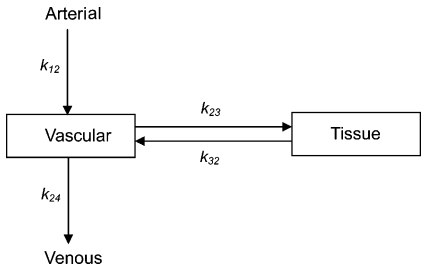

Figure 2. Structure of proposed model for IPPSF drug disposition, where k_{12}, k_{23}, k_{32}, and k_{24} are transfer rate constants.

Porcine skin is widely used for skin absorption and biodistribution studies because it is anatomically, physiologically, and biochemically similar to human skin.[24−28] The isolated perfused porcine skin flap (IPPSF), an alternative in vitro model, was developed to study xenobiotic percutaneous absorption of compounds. This model has been shown to predict absorption in humans,[29] has been used to study pharmacological effects on skin perfusion,[30] and is a useful model to directly quantitate tissue extraction following intra-arterial infusion,[31−33] the latter being its application in the present work.

Weanling Yorkshire pigs (20−30 kg) were acclimated for one week prior to surgery. Pigs were housed singly in an AALAC-accredited facility on an elevated floor and provided water (ad libitum) and 15% protein pellets. Two single-pedicle axial pattern skin flaps, each lateral to the ventral midline on the pig abdomen, were created and then harvested after 48 h.[34,35] The flaps were cannulated, flushed with heparinized saline, transferred to a temperature and humidity regulated chamber, and perfused for 1 h at a flow rate of 1.5 mL/h with a modified Krebs/Ringer's bicarbonate buffered media to ensure viability.[34] QD-PEG or QD-COOH at three concentrations (6.67, 3.33, or 1.67 nM,) were infused in media into the IPPSF for 4 h (dose phase), followed by an additional 4 h of media only perfusion (washout phase). Arterial and venous media was sampled to determine the glucose utilization and fluorescence assayed for QD quantitation. A total of 14 IPPSF were utilized with seven replicates per QD type. Following the washout phase, skin was harvested from the flap and fixed in Trumps' fixative at 4 °C for TEM. The skin flap was then cut into six segments and quickly frozen in liquid nitrogen at stored at −80 °C.

To quantitate QD fluorescence, arterial and venous media was aliquotted (200 μL; $n = 3$ wells) into 96-well black plates with microclear bottoms (Corning/Costar) and assayed on a tunable molecular dynamics Gemini EM (Molecular Devices Corporation, Sunnyvale, CA). The excitation/emission window was set at 360 nm/621 nm. Cadmium was also determined by inductively coupled plasma (ICP) emission spectrometry, which correlated to fluorescence ($R^2 = 0.81$).

Arterial−venous extraction data, reflecting QD remaining in the vascular system, were modeled by MATLAB using FMINSEARCH (weighted) with estimation of minimum parameters by optimally fitting the exponential curve. For comparing tissue disposition of QD-PEG fraction with QD-COOH, the observed input and output flux profiles were

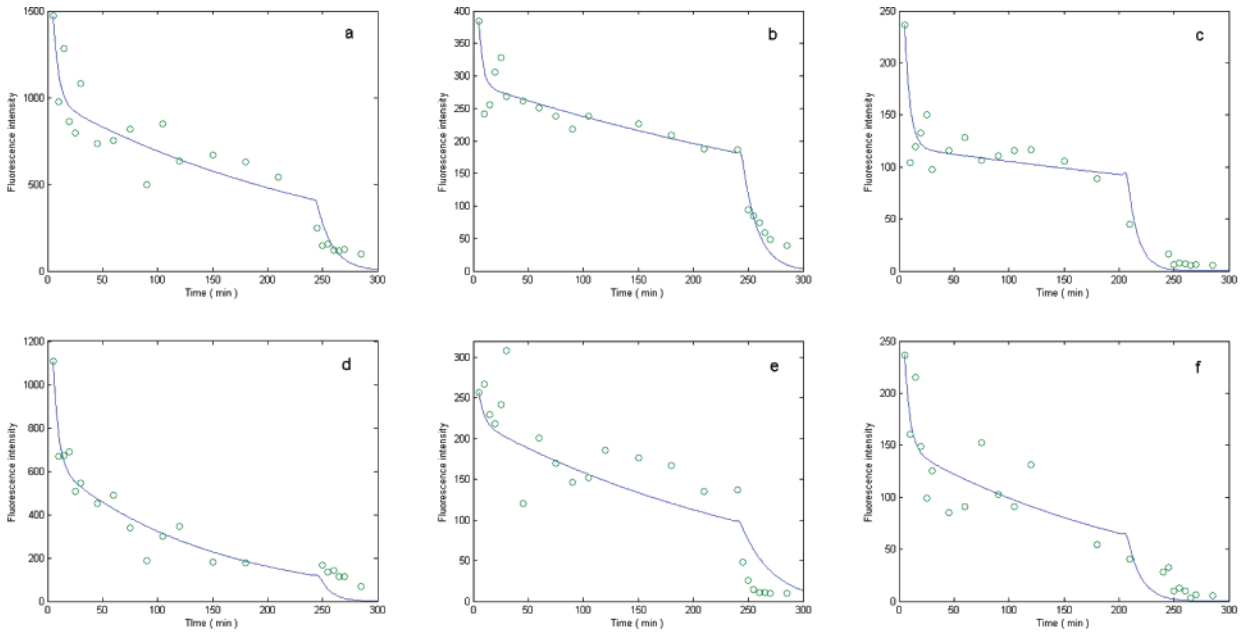

Figure 3. Normalized exponential curves of actual experimental data for three concentrations (6.67, 3.33, and 1.67 nM) for QD-PEG (a,b,c) and QD-COOH (d,e,f).

Table 1. Mean Estimated Parameters of QD-PEG and QD-COOH

	mean	
	PEG	COOH
$K(k_{12} - k_{24})$	0.0318	0.0724
k_{23}	0.0256	0.1401
k_{32}	0.0313	0.0641
k_{23}/k_{32}	0.8179	2.1856

fitted to a multicompartment model similar to that previously used to model platinum-based chemotherapeutics (Figure 2).[33]

Three first-order ordinary differential equations (ODE) were utilized that involved two dependent variables (vascular (Va) and tissue (T)) with three compartments, arterial (A)−venous (V), vascular (Va), and tissue (T), and one independent variable (time), that provides quantitative estimates of QD extraction into perfused tissue and vascular spaces. The assumptions are that rate constants are linear (not dependent on concentration) and all compartments are instantaneously stirred. An analytical solution to this model is presented in Supporting Information.

Figure 3 depicts exponential curves of three concentrations (6.67, 3.33, and 1.67 nM) for QD-PEG and QD-COOH in IPPSF. Between about 0 and 50 min of the dose phase, the AV profiles decayed rapidly. Oscillations were observed between 50 and 200 min. This pattern was followed by a rapidly decaying washout phase after 210 min.

Table 1 describes the estimated model parameters of QD-PEG and QD-COOH while Tables 2 and 3 tabulate actual experimental data. The mean is calculated by normalizing the data across infusion concentrations for seven IPPSF for each QD. The low SEM seen for each particle type across different infusion concentrations indicates linear extractions in this range of QD concentrations (1.67−6.67 nM). QD-PEG was significantly different than QD-COOH, with all estimated parameters of QD-COOH being greater than QD-PEG ($p < 0.05$). There is a greater QD-COOH fraction deposited in tissue ($k_{23} - k_{32} = 0.076$ min^{-1}) compared to QD-PEG ($k_{23} - k_{32} = -0.0057$ min^{-1}); a phenomenon also seen in the greater k_{23}/k_{32} ratio for COOH.

Table 2. Examples of Individual IPPSF Arterial−Venous Extractions at Three Infusion Concentrations (6.67, 3.33, and 1.67 nM)

	arterial−venous (fluorescence intensity)					
	PEG			COOH		
time	SF 3158	SF 3159	SF 3164	SF 3180	SF 3183	SF 3184
5	1472.5	384.6	236.6	1105.3	256.7	236.7
10	975.0	241.4	104.2	669.7	267.1	160.6
15	1281.2	255.4	119.6	672.8	230.1	215.4
20	862.1	305.8	132.4	690.1	218.1	148.8
25	794.4	328.0	150.4	505.4	242.1	98.9
30	1079.0	267.9	97.5	546.7	308.2	125.2
45	734.3	261.0	115.6	451.1	120.5	85.0
60	753.2	251.3	128.0	488.2	200.3	91.2
75	816.9	237.8	106.0	340.1	170.0	152.7
90	500.0	217.7	110.6	186.0	146.6	102.9
105	849.0	238.1	115.7	298.9	151.8	91.0
120	633.5	271.5	116.6	344.9	185.8	130.9
150	670.8	226.8	105.4	179.7	176.7	153.1
180	628.5	209.0	89.0	176.3	167.3	54.7
210	541.8	187.2	44.6	374.5	135.1	40.6
240	639.0	186.5	199.0	384.7	137.3	28.1

K that reflects the difference of arterial and venous concentrations remaining in the vascular compartment of QD-COOH (0.0724 min^{-1}) was greater than the QD-PEG (0.0318 min^{-1}). Also, this is demonstrated in the flux profiles in Figure 4, and confocal microscopy confirmed the model prediction of greater tissue deposition of the QD-COOH compared to QD-PEG in Figure 5.

Table 3. Calculated Mean Experimental Data of QD-PEG and QD-COOH in All 14 IPPSFs

	mean (A−V)			
time	PEG	SEM	COOH	SEM
5	1012.52	6.9	640.32	14.0
10	794.80	8.6	445.67	9.3
15	852.55	7.9	442.48	6.1
20	632.44	10.1	443.85	6.7
25	674.34	7.2	407.26	21.4
30	659.51	9.6	377.66	5.5
45	425.45	3.6	343.80	7.5
60	493.90	21.3	334.33	4.4
75	449.63	6.7	267.28	16.8
90	380.19	11.1	169.94	7.0
105	445.88	6.8	230.41	6.6
120	512.25	10.0	271.35	2.1
150	432.48	10.3	138.64	15.8
180	422.07	3.9	172.87	6.5
210	435.72	6.9	214.99	8.2
240	302.51	12.4	285.11	5.3

QD-COOH were present in greater quantity and accumulated in the capillaries. Previously, we have shown in human keratinocytes cell cultures that COOH-coated anionic QD had greater cellular uptake than the neutral PEG-coated QD.[14,15] These current studies extend this to coating-dependent biodistribution and cellular uptake in a more biologically complex perfused tissue model. Imaging studies in mice also showed that the QD surface coatings alter their disposition and pharmacokinetic properties.[13] Anionic maghemite nanoparticles have been shown to have excellent cellular uptake.[36] The advantage of using a pharmacokinetic approach as described herein is that the arterial extraction rate constants could be applied to any QD systemic blood concentrations obtained after extravascular exposure, even after inhalational, dermal, or oral absorption studies.

In Figure 4, we truncated the data points after 250 min for a more detailed analysis of the observed periodicity. This periodicity was well described by the periodic function that was similar across both QD types (period approximately 100 min). By computing the periodic function, the error was reduced. In Figure 4, the error of exponential curve was $\sqrt{4.5320\times10^4}$, while the error of the periodic curve was $\sqrt{2.6000\times10^3}$. This suggests that the periodic method accurately fitted the curve. This periodicity has never been seen in previous drug infusion IPPSF studies.[33] To assess this, we subjected archival drug infusion data to the same analysis as the QD described above.

Figure 6 depicts vascular concentrations of arterial−venous differences under four different chemical infusions of lidocaine, testosterone, cisplatin, and carboplatin. Oscillations were not evident in any of the plots. This was confirmed by MATLAB analysis of the errors of exponential versus periodic curve fits. Lidocaine and carboplatin infusion data did not have any evidence of periodicity to the degree that the periodic function of MATLAB could not be used. For testosterone and cisplatin, the errors of the periodic curves of both chemical infusions are higher than the exponential curves, suggesting that the exponential fitting method is more accurately fitting the curve.

Incorporation of this periodic function (sinusoidal (sine-like) function with an exponential decay; period length ≈ 100 min) into the base model significantly improved the model fit. The amplitude of this function, A in the periodic function equation ($f(t) = A \sin(Bt + C) + D$), was similar for PEG and COOH but decayed after 210 min. The essential of the amplitude test method is to measure the amplitudes of periods by fitting the observational QD-PEG and QD-COOH curves. The amplitude represents the contribution of the period to the QD curve, so it is the best criterion to decide on the importance of periods.

Of significance was the finding of a periodicity in the AV profiles across both types of QD and at all concentrations, a pattern not evident with chemical infusion studies in the IPPSF using the same experimental design for four different drugs. Temporal fluctuations in blood flow in the microcirculation show periodic tendencies caused by respiration and heart rate. These fluctuations can be described by a nonlinear mathematical model.[37] In the microvascular network, spontaneous oscillations are shown in about 30% vessels, while 70% of the vessels have steady flow according to Kiani's simulation.[38] Periodicity of the blood flow patterns, defined by oscillation, has even been suggested as a "sine qua non" of vasomotor activity,[37] although these vascular modulations are on a time scale of seconds. Oscillation is also a manifestation of inflammation in which the accumulation of white blood cells in the small vessels arrests the passage of blood, thus causing a redistribution of the blood driven by

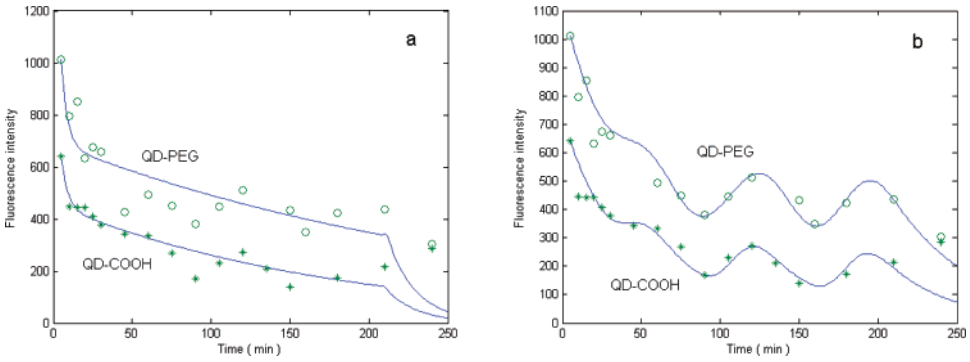

Figure 4. Combined fitting and periodic curves of mean data for QD-PEG and QD-COOH using the same experimental data points. The data points of (a) are fitted by nonlinear and exponential curve, and (b) is fitted by periodic curve.

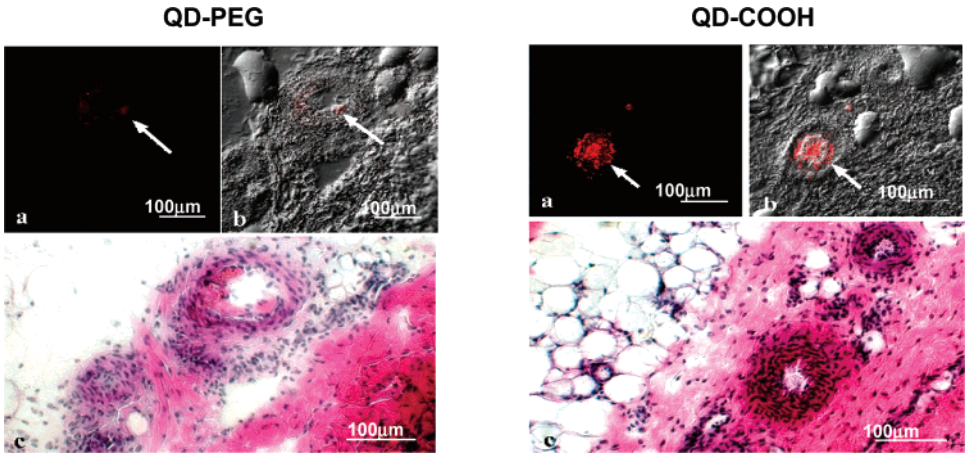

Figure 5. Laser scanning confocal microscopy: (a) confocal fluorescence image of QD deposition, (b) differential interference contrast (DIC) overlay depicting localization of QD in the capillary in the skin, (c) light micrograph of same area stained with hematoxylin and eosin for anatomical orientation. QD-PEG and QD-COOH infused in the IPPSF at a concentration of 3.33 nM. Arrows denote QD. Bars equal 100 μm.

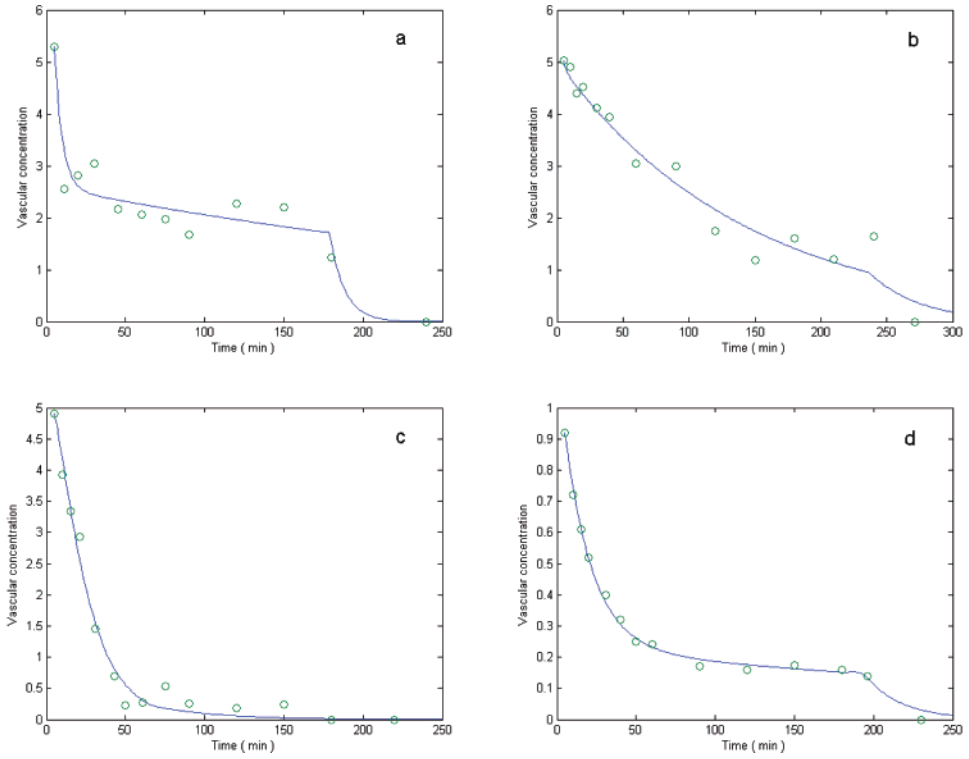

Figure 6. Normalized, predicted, and observed chemical infusion plots of intra-arterial IPPSF. (a) Lidocaine, (b) testosterone, (c) cisplatin, and (d) carboplatin. Their data points are fitted by a nonlinear exponential curve.

cardiac contraction. Braverman, using laser Doppler velocimetry in vivo in humans, demonstrated periodicity of erythrocyte flux between tissue beds having a period of approximately 90 min in humans.[39] This is of a similar order of magnitude to that seen with QD in the present study.

This periodicity would suggest an intriguing mechanism whereby QD modulate capillary bed perfusion. This phenomenon deserves further study to determine whether it is unique to QD or also occurs with other nanomaterials, if agglomeration and tissue binding is involved, or if it is a direct result of the pharmacological activity of QD that have entered capillary endothelial cells (Figure 5). What would be the application of such periodicity to nanoparticle biodistribution in vivo? Yang's study of QD 705 pharmacokinetics in mice after intravenous administration reported a time-dependent tissue redistribution from tissue masses (including skin) into the liver and kidneys,[17] a phenomenon that could be driven by such a periodicity in arterial extraction. These unique effects merit further research.

These results provide quantitative estimates of the magnitude of QD plasma to tissue distribution over a wide range of QD concentrations. The increase of QD-COOH extraction is consistent with previous cell culture data.[14,15] Finally, these analyses suggest a possible structure of mathematical models needed to predict nanomaterial biodistribution as well as identify a periodicity that may be related to local microvas-

cular tissue phenomenon not present in avascular in vitro model nor easily detected in more variable in vivo studies.

Acknowledgment. We thank Al Inman and James Brooks for technical assistance. This research is supported by the U.S. Environmental Protection Agency STAR Grant Program nos. RD 8317150 and 8514372.

Supporting Information Available: Description of confocal microscopy and analytical solution of mathematical model. This material is available free of charge via the Internet as http://pubs.acs.org.

References

(1) Jortner, J.; Rao, C. N. R. *Pure. Appl. Chem*. **2002**, *74*, 1491−1506.
(2) Zhan, G. D.; Kuntz, J. D.; Wan, J.; Mukherjee, A. K. *Nat. Mater.* **2003**, *2*, 38−42.
(3) Rajagopalan, P.; Wudl, F.; Schinazi, R. F.; Boudinot, F. D. *Antimicrob. Agents Chemother*. **1996**, *40*, 2262−2265.
(4) Qingnuam, L.; Yan, X.; Xiaodong, Z.; Ruili, L.; Qieqie, D.; Xiaoguang, S.; Shaoliang, C.; Wenxin, L. *Nucl. Med. Biol*. **2002**, *29*, 707−710.
(5) Riviere, J. E.; Tran, L. In *Nanotoxicology: Characterization, Dosing and Health Effects*; Monteiro-Riviere, N. A., Tran, L., Eds.; Informa: New York, 2007; pp 123−136.
(6) Cherukuri, P.; Gannon, C. J.; Leeuw, T. K.; Schmidt, H. K.; Smalley, R. E.; Curley, S. A.; Weisman, R. B. *Proc. Natl. Acad. Sci. U.S.A.* **2006**, *103*, 18882−18886.
(7) Liu, Z.; Cai, W.; He, L.; Nakayama, N.; Chen, K.; Sun, X.; Chen, X.; Dai, H. *Nat. Nanotechnol*. **2006**, *2*, 47−52.
(8) Singh, R.; Pantarotto, D.; Lacerda, L.; Pastorin, G.; Klumpp, C.; Prato, M.; Bianco, A.; Kostarelos, K. *Proc. Natl. Acad. Sci. U.S.A.* **2006**, *103*, 3357−3362.
(9) Oberdörster, G.; Oberdörster, E.; Oberdörster, J. *Environ. Health Perspect*. **2005**, *113*, 823−839.
(10) Oberdörster, G.; Maynard, A.; Donaldson, K.; Castranova, V.; Fitzpatrick; Ausman, K.; Carter, J.; Karn, B.; Kreyling, W.; Lai, D.; Olin, S.; Monteiro-Riviere, N.; Warheit, D.; Yang, H. *Part. Fibre Toxicol.* **2005**, *2*, 1−35.
(11) Michalet, X.; Pinaud, F. F.; Bentolila, L. A.; Tsay, J. M.; Doose, S.; Li, J. J.; Sundaresan, G.; Wu, A. M.; Gambhir, S. S.; Weiss, S. *Science* **2005**, *307*, 538−544.
(12) Chang, E.; Sun, J.; Miller, J. S.; Yu, W. W.; Colvin, V. L.; West, J. L.; Drezek, R. *Biochem. Biophys. Res. Commum*. **2005**, *334*, 1317−1321.
(13) Ballou, B.; Lagerholm, B. C.; Ernst, L. A.; Bruchez, M. P.; Waggoner, A. S. *Bioconjugate Chem.* **2004**, *15*, 79−86.
(14) Ryman-Rasmussen, J.; Riviere, J. E.; Monteiro-Riviere, N. A. *J. Invest. Dermatol.* **2007**, *127*, 143−153.
(15) Ryman-Rasmussen, J.; Riviere, J. E.; Monteiro-Riviere, N. A. *Nano Lett.* **2007**, *7*, 1344−1348.
(16) Chang, E.; Thekkek, N.; Yu, W. W.; Colvin, V. L.; Drezek, R. *Small* **2006**, *2*, 1412−1417.
(17) Yang, R. S. H.; Chang, L. W.; Wu, J. P.; Tsai, M. H.; Wang, H. J.; Kuo, Y. C.; Yeh, T. K.; Yang, C. S.; Lin, P. *Environ. Health Perspect.* **2007**.
(18) Yu, W. W.; Chang, E.; Drezek, R.; Colvin, V. L. *Biochem. Biophys. Res. Commum*. **2006**, *348*, 781−786.
(19) Yu, W. W.; Chang, E.; Falkner, C. J.; Zhang, J.; Al-Somali, A. M.; Sayes, C. M.; Johns, J.; Drezek, R.; Colvin, V. L. *J. Am. Chem. Soc.* **2007**, *129*, 2871 -2879.
(20) Li, J. J.; Wang, Y. A.; Guo, W.; Keay, J. C.; Mishima, T. D.; Johnson, M. B.; Peng, X. *J. Am. Chem. Soc.* **2003**, *125*, 12567−12575.
(21) Yu, W. W.; Qu, L.; Guo, W.; Peng, X. *Chem. Mater.* **2003**, *15*, 2854−2860.
(22) Yu, W. W.; Falkner, J. C.; Shih, B. S.; Colvin, V. L. *Chem. Mater.* **2004**, *16*, 3318−3322.
(23) Yu, W. W.; Falkner, J. C.; Yavuz, C. T.; Colvin, V. L. *Chem. Commun.* **2004**, *20*, 2306−2307.
(24) Monteiro-Riviere, N. A.; Stromberg, M. W. *Anat. Histol. Embryol*. **1985**, *14*, 97−115.
(25) Bissett, D. L.; McBride, J. F. In *Models in Dermatology I*; Maibach, H. I., Lowe, N. J., Eds.: Karger: Basel, 1985; pp 159−168.
(26) Monteiro-Riviere, N. A. In *Swine in Biomedical Research*; Tumbleson, M. E., Ed.; Plenum Publishing: New York, 1986; pp 641−655.
(27) Monteiro-Riviere, N. A.; Riviere, J. E. In *Advances In Swine In Biomedical Research*; Tumbleson, M. E., Schook, L. B., Eds.; Plenum Publishing: New York, 1996; pp 425−458.
(28) Monteiro-Riviere, N. A. In *The Biology of the Domestic Pig*; Pond, W. G., Mersmann, H. J., Eds.; Cornell University Press: Ithaca, NY, 2001; pp 625−652.
(29) Wester, R. C.; Melendres, J.; Sedik, L.; Maibach, H. I.; Riviere, J. E. *Toxicol. Appl. Pharmacol*. **1998**, *151*, 159−165.
(30) Rogers, R. A.; Riviere, J. E. *J. Pharm. Sci*. **1994**, *83*, 1682−1689.
(31) Vaden, S. L.; Page, R. L.; Peters, B. P.; Cline, J. M.; Riviere, J. E. *Cancer Res.* **1993**, *53*, 101−105.
(32) Williams, P. L.; Riviere, J. E. *Res. Commun. Chem. Pathol. Pharmacol.* **1988**, *66*, 145−158.
(33) Williams, P. L.; Riviere, J. E. *J. Pharm. Sci.* **1989**, *78*, 550−555.
(34) Monteiro-Riviere, N. A. In *Methods for Skin Absorption*; Kemppainen, B. W., Reifenrath, W. G., Eds.; CRC Press: Boca Raton, FL, 1990; pp 175−189.
(35) Bowman, K. F.; Dix, L. P.; Riond, J. L.; Riviere, J. E. *Am. J. Vet. Res.* **1986**, *47*, 1590−1596.
(36) Billotey, C.; Wilhelm, C.; Devaud, M.; Bacri, J. C.; Bittoun, J.; Gazeau, F. *Magn. Reson. Med.* **2003**, *49*, 646−654.
(37) Carr, R. T.; Lacoin, M. A. *Biomed. Eng*. **2000**, *28*, 641−652.
(38) Kiani, M. F.; Pries, A. R.; Hsu, L. L.; Sarelius, I. H.; Cokelet, G. L. *Am. J. Physics*. **1994**, *266*, H1822−H1828.
(39) Braverman, I. M.; Schechner, J. S. *J. Invest. Dermatol*. **1991**, *97*, 1013−1018.

NL071563C